Deuterium Kinetic Isotope Effects in Microsolvated Gas-Phase E2 Reactions

Nicole Eyet, Stephanie M. Villano, Shuji Kato, and Veronica M. Bierbaum

Department of Chemistry and Biochemistry, University of Colorado, Boulder, Colorado, USA

This work describes the first experimental studies of deuterium kinetic isotope effects (KIEs) for the gas-phase E2 reactions of microsolvated systems. The reactions of $F^-(H_2O)_n$ and $OH^-(H_2O)_n$, where $n = 0, 1$, with $(CH_3)_3CX$ (X = Cl, Br), as well as the deuterated analogs of the ionic and neutral reactants, were studied utilizing the flowing afterglow-selected ion flow tube technique. The E2 reactivity is found to decrease with solvation. Small, *normal* kinetic isotope effects are observed for the deuteration of the alkyl halide, while moderately *inverse* kinetic isotope effects are observed for the deuteration of the solvent. Minimal clustering of the product ions is observed, but there are intriguing differences in the nature and extent of the clustering process. Electronic structure calculations of the transition states provide qualitative insight into these microsolvated E2 reactions. (J Am Soc Mass Spectrom 2007, 18, 1046–1051)

The competing bimolecular nucleophilic substitution (S_N2) and bimolecular elimination (E2) reactions are some of the most widely studied reactions in organic chemistry. They have, for decades, been studied in solution, and more recently have been extensively studied in the gas phase as well [1–5]. Gas-phase studies allow for the examination of properties intrinsic to the reaction without contributions from solvent molecules.

Mass spectrometry is often used to explore such reactions in the gas phase [6]. However, since the ionic products resulting from a given set of reactants are usually the same for the competing pathways, directly monitoring these products often does not provide insight into the reaction mechanism. A few techniques have been used to distinguish the two mechanisms. Collection and detection of the neutral products is possible in some cases [7]. The use of dianionic nucleophiles can allow for the direct detection of two distinct ionic products that identifies the mechanism [8]. Alternatively, deuterium kinetic isotope effects (KIEs) have allowed for the study of competition between S_N2 and E2 mechanisms [2, 3, 9]. Deuterium KIEs are the ratio of the perprotio to the perdeutero rate constants (KIE $\equiv k_H/k_D$.) These effects are primarily due to changes in vibrational modes as a reaction proceeds from the reactants to the transition-state structure. A normal KIE (>1) is observed as a result of the loosening of bonds in the transition state, which causes a decrease in the difference of zero point energy, and is usually indicative of an E2 mechanism. An inverse KIE (<1) results from the tightening of bonds in the transition-state, causing an increase in zero point energy, characteristic of an S_N2 mechanism.

Even though condensed and gas-phase organic reactions are relatively well understood, the relationship between these two processes is not well defined. A study of microsolvated ions may shed light on the transition between these phases. Clearly, a single solvent molecule does not mimic solution-phase chemistry as a whole; however, the dynamics of an anion solvated with a single molecule can be similar to that of an anion in solution. Computational studies of S_N2 reactions show that in sufficiently exothermic reactions, the solvent molecules remain attached to the anion up to the transition state and, therefore, microsolvated systems are good approximate models for solution phase chemistry [10–12]; this is likely the case for exothermic E2 reactions as well.

Reactions involving microsolvated systems that proceed through an S_N2 pathway have been studied both experimentally and theoretically [10, 12–16]. For reactions of $F^-(H_2O)$ with methyl halides, O'Hair et al. [17] observed moderately inverse KIEs upon deuteration of the alkyl halide, and more substantial inverse KIEs upon deuteration of the solvent. Hu and Truhlar [10] computationally studied the reaction of $F^-(H_2O)$ with CH_3Cl, and their results are in excellent agreement with experiment. Kato et al. [18] expanded the experimental work by examining the reactions of $F^-(HF)$ and $F^-(CH_3OH)$ with methyl halides. Small to moderate inverse KIEs were reported for deuteration of the methyl halide. Perdeuteration of the solvent resulted in substantially inverse KIEs, while selective deuteration of the methanol solvent resulted in moderately inverse KIEs. Studies of microsolvated reactions that proceed

Address reprint requests to Dr. Veronica Bierbaum, Department of Chemistry and Biochemistry, University of Colorado, 215 UCB, Boulder, CO, 80309-0215, USA. E-mail: Veronica.Bierbaum@Colorado.edu

1044-0305/07/$32.00
doi:10.1016/j.jasms.2007.02.016

Published online April 19, 2007
Received December 15, 2006
Accepted February 28, 2007

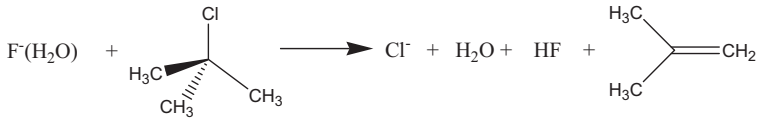

Scheme 1. E2 reaction of a t-butyl halide with a nucleophile. Although unclustered products are shown, the formation of clustered products is energetically favored.

via an E2 pathway have been lacking. To date, there have been no experimental studies of these types of systems, and only a few theoretical studies have been carried out. Bickelhaupt et al. [19] theoretically studied the microsolvated E2 transition sates for $F^-(HF)_n$ + $C_2H_5F(HF)_m$ reactions. Anti-elimination was found to be energetically favored over syn-elimination, as observed experimentally for bare ion systems; significant increases in the transition-state barriers are predicted upon microsolvation, resulting in the S_N2 pathway becoming more favorable than the E2 pathway. Wu and Hu [20] examined the E2 reaction dynamics and isotope effects for the reaction of $FO^-(H_2O)$ with ethyl chloride. Substantial normal kinetic isotope effects were calculated for the deuteration of ethyl chloride, and moderately inverse isotope effects were predicted for the deuteration of the solvent. For this reaction, the barrier height for the reaction is sufficiently greater than the entrance channel, and tunneling played a substantial role in the isotope effects.

Elimination reactions are favored over substitution reactions when steric factors affect reaction efficiency [21]. In the present work, t-butyl halides were chosen as the neutral reagent to examine E2 processes. A typical reaction is shown in Scheme 1.

Experimental

These reactions were carried out in a flowing afterglow-selected ion flow tube (FA-SIFT) [22]. Hydroxide is produced by electron impact on N_2O resulting in O^-, which then reacts with CH_4 by H-atom abstraction. Fluoride is produced by electron impact on NF_3. These bare ions are solvated by reaction with a mixture of either H_2O or D_2O in tetrahydrofuran [23]. The desired reactant ions were mass-selected using a quadrupole mass filter and injected into the reaction flow tube where they were thermally equilibrated to room temperature through collisions with He buffer gas (0.5 torr). A known flow of neutral reactants, measured by a calibrated volume technique, was added to the reaction flow tube through a series of inlets. The depletion of the reactant ion and formation of the product ions were monitored using the detection quadrupole mass filter coupled to an electron multiplier. The reactions were carried out at 301 ± 3 K. Parallel reactions of deuterated reactants were carried out under identical conditions.

Absolute uncertainties in these rate measurements are ±20%. Systematic errors cancel in the rate constant ratio, so that the error bars for KIEs are significantly smaller. Neutral reagents were obtained from commercial sources and used without further purification. [$(CH_3)_3CCl$ 98%, $(CH_3)_3CBr$ 96%, $(CD_3)_3CCl$ 99% D, $(CD_3)_3CBr$ 98% D, NF_3 99.7%, D_2O 99.9% D)] Helium buffer gas (99.995%) was purified by passage through a molecular sieve trap immersed in liquid nitrogen.

It was necessary to correct data for isobaric ions, mass discrimination, and ~15% bare ion formed due to collision-induced dissociation (CID) upon injection of clustered ions into the flow tube. Isobaric anions were present in the reactions of $OH^-(H_2O)$ and $F^-(H_2O)$ with both perprotio and perdeutero t-butyl chloride. Both $OH^-(H_2O)$ and $^{35}Cl^-$ have m/z = 35 and $F^-(H_2O)$ and $^{37}Cl^-$ have m/z = 37. The natural isotopic abundances of chlorine allowed for the correction of isobaric ions. Efforts were made to minimize mass discrimination. Estimates of the remaining mass discrimination were carried out through a series of calibration reactions. These reactions were chosen such that a single reactant ion, when allowed to react with a carefully chosen neutral reagent, resulted in a single product ion. Both reactant and product ions were chosen to be similar in mass to those that were studied in the E2 reaction. Correction for the bare ion present as a result of CID was necessary since its reaction with a t-butyl halide also formed product ions. This complication was accounted for by monitoring both reactants as a function of time and subtracting the bare ion contribution from the overall result.

Electronic structure calculations were carried out using the Gaussian 03 [24] and Gaussian 98 [25] program packages. Optimized geometries and frequencies of the reactants and the transition states were calculated using both ab initio methods (MP2/6-31 + G*) and density functional theory (B3LYP/6-311 ++ G**). These levels of theory were chosen because they have been shown to represent a compromise between cost and accuracy [26–29]. Cartesian coordinates of all optimized geometries, as well as energies of the transition-state structures, are provided in the Supporting Information (which can be found in the electronic version of this article). Transition states were identified as having exactly one imaginary frequency and by confirmation of movement along the reaction coordinate by animation of this frequency. Results of electronic structure calculations are used in this work for qualitative arguments only; a more thorough computational study is beyond the scope of this paper.

Table 1. E2 reaction rate constants, kinetic isotope effects, and products

Reaction	k_{E2} (10^{-10} cm^3 s^{-1})	k_{E2}/k_{col}	Neutral k_H/k_D	Solvent k_H/k_D	E2 products formed	Cluster branching fraction[a]
$OH^- + (CH_3)_3CCl$	25.5 ± 0.1	0.72	1.06 ± 0.03		Cl^-	
$OH^- + (CD_3)_3CCl$	24.1 ± 0.1	0.69			Cl^-	
$OH^-(H_2O) + (CH_3)_3CCl$	9.51 ± 0.38	0.36	1.38 ± 0.06	0.90 ± 0.05	Cl^-	
$OH^-(H_2O) + (CD_3)_3CCl$	6.89 ± 0.12	0.26		0.79 ± 0.02	Cl^-	
$OD^-(D_2O) + (CH_3)_3CCl$	10.5 ± 0.4	0.41	1.20 ± 0.05		Cl^-	
$OD^-(D_2O) + (CD_3)_3CCl$	8.77 ± 0.16	0.35			Cl^-	
$F^- + (CH_3)_3CCl$	25.3 ± 0.9	0.75	0.98 ± 0.07		Cl^-	
$F^- + (CD_3)_3CCl$	25.7 ± 1.6	0.77			Cl^-	
$F^-(H_2O) + (CH_3)_3CCl$[b]	0.878 ± 0.044	0.034	1.49 ± 0.13	0.87 ± 0.10	Cl^-; Cl^-(HF)	0.67
$F^-(H_2O) + (CD_3)_3CCl$[b]	0.590 ± 0.041	0.023		0.85 ± 0.08	Cl^-; Cl^-(DF)	0.50
$F^-(D_2O) + (CH_3)_3CCl$[b]	1.01 ± 0.10	0.040	1.46 ± 0.17		Cl^-; Cl^-(HF)	0.77
$F^-(D_2O) + (CD_3)_3CCl$[b]	0.695 ± 0.045	0.028			Cl^-; Cl^-(DF)	0.54
$OH^- + (CH_3)_3CBr$	26.6 ± 0.7	0.70	1.10 ± 0.07		Br^-	
$OH^- + (CD_3)_3CBr$	24.1 ± 1.4	0.64			Br^-	
$OH^-(H_2O) + (CH_3)_3CBr$	16.0 ± 0.7	0.57	1.04 ± 0.10	0.81 ± 0.04	Br^-	
$OH^-(H_2O) + (CD_3)_3CBr$	15.5 ± 1.4	0.56		0.78 ± 0.90	Br^-	
$OD^-(D_2O) + (CH_3)_3CBr$	19.8 ± 0.2	0.73	1.00 ± 0.06		Br^-	
$OD^-(D_2O) + (CD_3)_3CBr$	19.8 ± 1.3	0.74			Br^-	
$F^- + (CH_3)_3CBr$	25.8 ± 0.4	0.71	1.06 ± 0.08		Br^-	
$F^- + (CD_3)_3CBr$	24.5 ± 1.8	0.68			Br^-	
$F^-(H_2O) + (CH_3)_3CBr$	15.0 ± 0.3	0.55	1.21 ± 0.14	0.94 ± 0.06	Br^-; Br^-(HF); $Br^-(H_2O)$	0.13[c]
$F^-(H_2O) + (CD_3)_3CBr$	12.4 ± 1.4	0.46		0.92 ± 0.11	Br^-; Br^-(DF); $Br^-(H_2O)$	0.25[c]
$F^-(D_2O) + (CH_3)_3CBr$	15.9 ± 0.9	0.59	1.19 ± 0.09		Br^-; Br^-(HF); $Br^-(D_2O)$	0.17[c,d]
$F^-(D_2O) + (CD_3)_3CBr$	13.4 ± 0.6	0.50			Br^-; Br^-(DF); $Br^-(D_2O)$	0.26[c]

[a]Errors in branching fractions are estimated to be ±50% due to correction for mass discrimination and the presence of ~15% F^- reactant anion from collisional dissociation of the solvated anion upon injection.
[b]Reactions of water-solvated fluoride with t-butyl chloride also led to an association product. This contribution has been removed from the total rate constant to produce the tabulated rate constants, and from the total branching ratio to produce the tabulated branching ratios. Total rate constants are: $F^-(H_2O) + (CH_3)_3CCl$ $k_{total} = 0.971 \times 10^{-10}$cm^3 s^{-1}; $F^-(H_2O) + (CD_3)_3CCl$ $k_{total} = 0.768 \times 10^{-10}$cm^3 s^{-1}; $F^-(D_2O) + (CH_3)_3CCl$ $k_{total} = 1.19 \times 10^{-10}$cm^3 s^{-1}; $F^-(D_2O) + (CD_3)_3CCl$ $k_{total} = 0.926 \times 10^{-10}$ cm^3 s^{-1}. Association branching fractions are 0.10, 0.23, 0.15, and 0.25, respectively.
[c]The reactions with t-butyl bromide produce both water-solvated and hydrogen fluoride-solvated anions. The reported branching fraction represents the sum of these clusters. Hydrogen fluoride-solvated anions are between two and three times as abundant as water-solvated anions.
[d]Both $Br^-(D_2O)$ and Br^-(HF) have m/z = 99 and 101.

Results and Discussion

Table 1 summarizes the rate constants, reaction efficiencies, and products of bare and solvated hydroxide and bare and solvated fluoride reacting with t-butyl chloride and t-butyl bromide, as well as deuterated analogs of the ionic and neutral reagents. Reported rate constants are the average of at least three individual measurements. The reaction efficiency is defined as the ratio of the experimentally determined rate constant to the collisional rate constant; the latter values were determined using parameterized trajectory collision rate theory [30]. Electric dipole polarizabilities for both t-butyl chloride and t-butyl bromide were calculated using the Miller-Savchik method [31], and were found to be 9.91 × 10^{-24} cm^3 and 10.8 × 10^{-24} cm^3, respectively. The permanent dipole moment for t-butyl chloride was taken from Lide [32] as 2.130 D. The dipole moment for t-butyl bromide was calculated using the Gaussian 03 program package [24] as 2.596 D. This calculation also confirmed the electric dipole polarizability of t-butyl bromide.

The displaced halide ion is the sole ionic product of the reactions with unsolvated ions. Additionally, reactions with $OH^-(H_2O)$ and $OD^-(D_2O)$ produce only the bare, displaced halide ion. In contrast, the reactions of $F^-(H_2O)$ and $F^-(D_2O)$ with $(CH_3)_3CCl$ produce Cl^-, Cl^-(HF), and an association complex, $F^-(H_2O, D_2O)((CH_3)_3CCl)$. Deuteration of the alkyl halide results in Cl^-(DF) clusters. The branching fractions for the association products were subtracted from the total reactivity in determining the intrinsic E2 reaction rates. The reactions of $F^-(H_2O)$ and $F^-(D_2O)$ with $(CH_3)_3CBr$ produce Br^-, Br^-(HF), and $Br^-(H_2O)$ or $Br^-(D_2O)$. No association products are formed in this series of reactions. Deuteration of the alkyl halide results in Br^-(DF). These product branching ratios are also summarized in Table 1, and the reaction energetics are given in Table 2.

Kinetic Isotope Effects

The kinetic isotope effects studied here can be considered in two groups; first, the KIEs due to the deuteration of the t-butyl halide, and second, the KIEs due to the deuteration of the reactant anion. These effects are multiplicative [17, 18]; the KIE for the overall perdeutero reaction is the product of the KIE for the perdeutero alkyl halide reaction and the perdeutero solvent reaction.

Table 2. E2 reaction energetics[a]

Reaction	Ionic product	ΔH_{rxn} (kJ/mol)	ΔG_{rxn} (kJ/mol)
$OH^- + (CH_3)_3CCl$	Cl^-	−177	−220
$OH^-(H_2O) + (CH_3)_3CCl$	Cl^-	−63	−141
	$Cl^-(H_2O)$	−126	−176
$F^- + (CH_3)_3CCl$	Cl^-	−94	−142
$F^-(H_2O) + (CH_3)_3CCl$	Cl^-	18	−50
	$Cl^-(HF)$	−73	−113
	$Cl^-(H_2O)$	−44	−85
$OH^- + (CH_3)_3CBr$	Br^-	−209	−247
$OH^-(H_2O) + (CH_3)_3CBr$	Br^-	−95	−164
	$Br^-(H_2O)$	−149	−203
$F^- + (CH_3)_3CBr$	Br^-	−127	−173
$F^-(H_2O) + (CH_3)_3CBr$	Br^-	−14	−82
	$Br^-(HF)$	−85	−127[b]
	$Br^-(H_2O)$	−67	−112

[a]Data to determine ΔH_{rxn} and ΔG_{rxn} were taken from the JANAF Thermochemical Tables [33] or the NIST WebBook [34].
[b]The entropy of $Br^-(HF)$ was estimated by analogy to other clustered anions.

$$KIE = \frac{k[F^-(H_2O) + (CH_3)_3CCl]}{k[F^-(D_2O) + (CD_3)_3CCl]} = \frac{k[F^-(H_2O) + (CH_3)_3CCl]}{k[F^-(H_2O) + (CD_3)_3CCl]} \times \frac{k[F^-(H_2O) + (CH_3)_3CCl]}{k[F^-(D_2O) + (CH_3)_3CCl]}$$

This result supports the approximation that the effects can be discussed separately.

For reactions that are sufficiently exothermic, rate constants approach their collision-controlled limits. For reactions that are less exothermic, E2 reactivity is found to increase with increasing exothermicities. In general, when considering reactions below the collision controlled limits, the reactions of t-butyl bromide are more rapid than those with t-butyl chloride, and reactions of $OH^-(H_2O)_n$ are more rapid than those of $F^-(H_2O)_n$, where $n = 0, 1$. Reaction rates of solvated anions are slower than for bare anions, as observed for S_N2 reactions [16, 35]. Specifically, the measured reaction rates are a factor of about three slower for solvated OH^- reacting with t-butyl chloride when compared to bare OH^-. Reaction rates were found to be a factor of about 30 slower for the reactions of t-butyl chloride with solvated F^- when compared with bare F^-. In reactions with t-butyl bromide, rates of reactions were a factor of about 2 slower for all solvated ions in comparison to their bare counterparts.

Since the reaction efficiencies of both t-butyl halides with either bare ion are large, approaching saturation, it is expected that the intrinsic differences in their transition states are not reflected in the measured KIEs. The isotope effects measured for the bare ions approach unity. The reaction efficiencies of the solvated anion reactions, however, do not approach saturation. These KIEs should accurately reflect the differences in transition states of the perprotio and perdeutero reactants, especially for the $F^-(H_2O) + (CH_3)_3CCl$ reactions. Reactions of $F^-(H_2O)$ with t-butyl chloride and their deuterated counterparts are least efficient and the isotope effects are the largest of the series. Reactions of $OH^-(H_2O)$ with t-butyl chloride and the reactions of $F^-(H_2O)$ with t-butyl bromide display intermediate kinetic isotope effects. The isotope effects are the smallest for $OH^-(H_2O)$ reacting with t-butyl bromide, which are the fastest of the solvated ion reactions. Overall, the most striking observation is that all of the isotope effects are relatively small. Typical solution phase E2 kinetic isotope effects are between 2 and 6 [36].

One possible explanation for the small isotope effects could be that the reaction proceeds through both an S_N2 and E2 mechanism. A comprehensive theoretical study [19] of the effects of microsolvation on E2 and S_N2 systems, specifically the reaction of ethyl fluoride with fluoride anion, has found that microsolvated systems should react preferentially via the S_N2 pathway. Increasing the solvation of the system was shown to stabilize the S_N2 transition-state relative to the anti-E2 transition-state. This study, however, concentrated on reactions of ethyl fluoride for which the steric hindrance is small toward the Walden inversion so that the S_N2 pathway is already competitive for bare nucleophiles.

Our previous study [21] suggests that ethyl halides can react through both S_N2 and E2 pathways. It was observed that for a series of alkyl halides (methyl through t-butyl) reacting with sulfur anions, the rate constant decreased dramatically with increasing α-branching. For reactions of the same series of alkyl halides with oxy-anions or fluoride, the rate constants increase with increased α-branching of the alkyl group; that is, the reactions of these nucleophiles with a t-butyl halide were faster than the reaction with a methyl halide. These results demonstrated that sulfur anions react almost exclusively via an S_N2 process and the increased steric hindrance reduces the reaction rate. For oxy-anions and fluoride, reactions proceed through an E2 channel, even when the S_N2 channel is thermodynamically allowed. For these reactions, it was seen that the E2 process is important with molecules as small as ethyl halides and occurs almost exclusively for isopropyl and t-butyl halides, as also suggested from the kinetic isotope effects in the ClO^- reactions [2, 3]. It is expected that even if the S_N2 transition-state is more stabilized upon microsolvation, the inherent steric hindrance will still control the reaction pathway for the t-butyl system in favor of the E2 channel.

In addition, the detection of HF and DF clusters as products in the reactions of $F^-(H_2O)$ with perprotio and perdeutero t-butyl chloride, respectively, also provides evidence that these reactions proceed at least partially through an E2 mechanism. Likely the reactions with $OH^-(H_2O)$ proceed in an analogous way.

It may be possible that other mechanisms are contributing to the measured reaction rate. Viggiano et al.

[16] have observed ligand switching followed by thermal dissociation, rather than an anticipated S_N2 process, in the reactions of $Cl^-(H_2O)$ with CH_3Br. Although ligand switching is mechanistically possible for our reactions, it is unlikely because we see no evidence of ligand switching products. In addition, the S_N2 pathways for the reactions studied by Viggiano and coworkers are endothermic and switching should occur only for weakly bound hydrates. The reactions studied here are exothermic and involve strongly bound hydrates, making the ligand switching channel significantly energetically unfavorable.

Since it is unlikely that the small isotope effects can be attributed to a contribution from an alternative mechanism, these studies suggest the occurrence of an early transition-state due to the large reaction exothermicities. The solvated reactions with $OH^-(H_2O)$ and $F^-(H_2O)$ in the present study are both sufficiently exothermic. Since the KIEs reflect the difference in zero point energies between the reactant complex and the transition state, small changes in the geometries and, hence, the zero point energies would result in small KIEs.

The solvent KIEs, as summarized in Table 1, are moderately inverse and consistent with our previous results for solvated S_N2 reactions [17, 18]. This effect is attributed to a decrease in bond length within the solvent molecule in the transition state, relative to those bonds in the reactant ion. This result was shown computationally for the S_N2 reaction of $F^-(H_2O)$ with CH_3Cl, [10] as well as for the E2 contribution to the reaction of $FO^-(H_2O) + C_2H_5Cl$ [20]. Our electronic structure calculations also show a substantial decrease in the water bond length when comparing the transition states with the reactants.

Reaction Dynamics

The reactions of $F^-(H_2O)$ with t-butyl chloride produce comparable amounts of Cl^- and $Cl^-(HF)$, and the association product is a minor product. The reactions of $F^-(H_2O)$ with t-butyl bromide produce Br^- as the major product, and $Br^-(HF)$ and $Br^-(H_2O)$ are identified as minor products. While clearly entropic factors will favor the production of unclustered products, these contributions are small. The overall energetics of these reactions, as shown in Table 2, are dominated by enthalpy contributions and suggest that the formation of clustered products will dominate the product distribution. While entropic effects may explain why a significant amount of unclustered chloride forms from the endothermic reaction with t-butyl chloride, it is most likely reaction dynamics that define the product distribution.

The calculated transition states show that the antiperiplanar geometry is significantly energetically favored over the syn-periplanar geometry. These trends are the same for both ab initio and density functional theory calculations. If the product dynamics are more direct than statistical, this transition-state geometry may hinder the formation of clusters as a major product. The t-butyl group lies between the leaving halide and the newly formed elimination product, sterically hindering the formation of the clusters.

Likely, the preference to form bare anions and the varied distribution of clustered products is due to product dynamics in the posttransition-state reaction complex [37]. Without a comprehensive computational study, it is possible to offer only a qualitative assessment. In order for a reaction to be statistical, complete randomization of energy through intramolecular vibrational redistribution (IVR) must occur [38]. This situation requires that vibrational mode coupling be intrinsically efficient and also that the posttransition-state complex be sufficiently long-lived. Reactions of $OH^-(H_2O)$ are highly exothermic and they may not allow for complete IVR in the posttransition-state regime. If nonstatistical dynamics do contribute to this reaction it would explain the lack of clustered products. The reactions with $F^-(H_2O)$ are significantly less exothermic than those of $OH^-(H_2O)$. The difference in these product distributions may be related to the different complex lifetimes in the posttransition-state regime.

Additionally, incomplete IVR in the postreaction complex could explain the difference in product distribution between the t-butyl chloride and t-butyl bromide reactions, for which the reaction exothermicities are relatively similar (Table 2). In general, heavier systems have more low-frequency vibrational modes that would facilitate more efficient vibrational coupling. The enhanced mode mixing, along with the greater density of states, also increases the complex lifetime. If this is the case, the heavier t-butyl bromide complexes would be the longest lived. Therefore, the more statistical nature of these reactions leads to clustering with both HF and H_2O. Since $Br^-(HF)$ is the more strongly bound cluster when compared with $Br^-(H_2O)$, its formation is more favorable and dominates the clustered product distribution.

By comparing the perprotio and perdeutero anion reactions within each series, it is seen that the heavier complex yields a larger amount of clustered products. The same is true for the perprotio and perdeutero t-butyl bromide species. The branching fraction for the total clusters formed in the t-butyl bromide reaction is significantly smaller than the clustered product branching ratio for the t-butyl chloride reactions. Presumably, this is due to the strength of the interaction between Cl^- and HF when compared with the interactions between Br^- and either HF or H_2O.

Conclusions

Microsolvated E2 reactions were studied using deuterium kinetic isotope effects. Isotope effects for deuteration of the t-butyl halide tend to increase with decreasing reaction efficiency. The small normal isotope effects are attributed to an early transition-state in which the geometries do not change significantly between the reactant complex and the transition-state. Isotope effects for deuteration of the sol-

vated anion are moderately inverse. Changes in the water bond length within the solvent produce these effects, and more dramatic decreases in the bond length produce a more inverse effect.

The distribution of product ions is rationalized by the calculated transition-state structures and the subsequent reaction dynamics. The product dynamics of t-butyl bromide and $F^-(H_2O)$ appear most statistical and therefore allow for the production of Br^- as well as $Br^-(HF)$ and $Br^-(H_2O)$. The dynamics of both t-butyl halides with $OH^-(H_2O)$ appear most direct, and the only products are bare halide ions. The reaction of t-butyl chloride with $F^-(H_2O)$ likely represents an intermediate case. A full computational and dynamical study is necessary to completely understand these results. In addition, more experimental studies are planned to further elucidate the transition between gas and condensed phase for these prototypical E2 reactions.

Acknowledgments

The authors gratefully acknowledge support from the National Science Foundation (CHE-0349937). Electronic structure calculations were performed using the JILA Keck cluster, for which the authors acknowledge support from the W. M. Keck Foundation. Additionally, the authors thank John Stanton for helpful discussions.

References

1. Wladkowski, B. D.; Brauman, J. I. Substitution Versus Elimination in Gas-Phase Ionic Reactions. *J. Am. Chem. Soc.* **1992,** *114*, 10643–10644.
2. Villano, S. M.; Kato, S.; Bierbaum, V. M. Deuterium Kinetic Isotope Effects in Gas-Phase S_N2 and E2 Reactions: Comparison of Experiment and Theory. *J. Am. Chem. Soc.* **2006,** *128*, 736–737.
3. Hu, W.-P.; Truhlar, D. G. Factors Affecting Competitive Ion-Molecule Reactions: ClO^- + C_2H_5Cl and C_2D_5Cl via E2 and S_N2 Channels. *J. Am. Chem. Soc.* **1996,** *118*, 860–869.
4. de Koning, L. J.; Nibbering, N. M. M. On the Mechanism of Base-Induced Gas-Phase Elimination Reactions of Ethers. *J. Am. Chem. Soc.* **1987,** *109*, 1715–1722.
5. Gronert, S. Mass Spectrometric Studies of Organic Ion/Molecule Reactions. *Chem. Rev.* **2001,** *101*, 329–360.
6. Munsch, T. E.; Wenthold, P. G. Organic Gas-Phase Ion Chemistry. *Annu. Rep. Prog. Chem B* **2003,** *99*, 420–446.
7. Jones, M. E.; Ellison, G. B. Gas-Phase E2 Reactions: Methoxide Ion and Bromopropane. *J. Am. Chem. Soc.* **1989,** *111*, 1645–1654.
8. Gronert, S. Gas Phase Studies of the Competition Between Substitution and Elimination Reactions. *Acc. Chem. Res.* **2003,** *36*, 848–857.
9. Gronert, S.; DePuy, C. H.; Bierbaum, V. M. Deuterium Isotope Effects in Gas-Phase Reactions of Alkyl Halides: Distinguishing E2 and S_N2 Pathways. *J. Am. Chem. Soc.* **1991,** *113*, 4009–4010.
10. Hu, W.-P.; Truhlar, D. G. Modeling Transition State Solvation at the Single-Molecule Level: Test of Correlated ab Initio Predictions against Experiment for the Gas-Phase S_N2 Reaction of Microhydrated Fluoride with Methyl Chloride. *J. Am. Chem. Soc.* **1994,** *116*, 7797–7800.
11. Tachikawa, H. Collision Energy Dependence on the Microsolvated S_N2 Reaction of $F^-(H_2O)$ with CH_3Cl: A Full Dimensional Ab Initio Direct Dynamics Study. *J. Phys. Chem. A* **2001,** *105*, 1260–1266.
12. Ohta, K.; Morokuma, K. An MO study of S_N2 Reactions in Hydrated Gas Clusters: Hydrated Hydroxide $[(H_2O)_nOH^-]$ + Hydrated Methyl Chloride $[MeCl(H_2O)_m]$ → methanol + chloride + (n + m)water. *J. Phys. Chem.* **1985,** *89*, 5845–5849.
13. Seeley, J. V.; Morris, R. A.; Viggiano, A. A. Temperature Dependencies of the Rate Constants and Branching Ratios for the Reactions of $F^-(H_2O)_{0-5}$ with CH_3Br. *J. Phys. Chem. A* **1997,** *101*, 4598–4601.
14. Takashima, K.; Riveros, J. M. Gas-Phase Solvated Negative Ions. *Mass Spectrom. Rev.* **1999,** *17*, 409–430.
15. Tucker, S. C.; Truhlar, D. G. Effect of Nonequilibrium Solvation on Chemical Reaction Rates. Variational Transition-State-Theory Studies of the Microsolvated Reaction $Cl^-(H_2O)_n$ + CH_3Cl. *J. Am. Chem. Soc.* **1990,** *112*, 3347–3361.
16. Viggiano, A. A.; Arnold, S. T.; Morris, R. A. Reactions of Mass-Selected Cluster Ions in a Thermal Bath Gas. *Int. Rev. Phys. Chem.* **1998,** *17*, 147–184.
17. O'Hair, R. A. J.; Davico, G. E.; Hacaloglu, J.; Dang, T. T.; DePuy, C. H.; Bierbaum, V. M. Measurements of Solvent and Secondary Kinetic Isotope Effects for the Gas-Phase S_N2 Reactions of Fluoride with Methyl Halides. *J. Am. Chem. Soc.* **1994,** *116*, 3609–3610.
18. Kato, S.; Hacaloglu, J.; Davico, G. E.; DePuy, C. H.; Bierbaum, V. M. Deuterium Kinetic Isotope Effects in the Gas-Phase S_N2 Reactions of Solvated Fluoride Ions with Methyl Halides. *J. Phys. Chem. A* **2004,** *108*, 9887–9891.
19. Bickelhaupt, F. M.; Baerends, E. J.; Nibbering, N. M. M. The Effect of Microsolvation on E2 and S_N2 Reactions: Theoretical Study of the Model System F^- + C_2H_5F + nHF. *Chem. Eur. J.* **1996,** *2*, 196–207.
20. Wu, Y.-R.; Hu, W.-P. Reaction Dynamics Study on the Tunneling Effects of a Microsolvated E2 Reaction: $FO^-(H_2O)$ + C_2H_5Cl → $HOF(H_2O)$ + C_2H_4 + Cl^-. *J. Am. Chem. Soc.* **1999,** *121*, 10168–10177.
21. DePuy, C. H.; Gronert, S.; Mullin, A.; Bierbaum, V. M. Gas-Phase S_N2 and E2 Reactions of Alkyl Halides. *J. Am. Chem. Soc.* **1990,** *112*, 8650–8655.
22. Van Doren, J. M.; Barlow, S. E.; DePuy, C. H.; Bierbaum, V. M. The Tandem Flowing Afterglow-SIFT-Drift. *Int. J. Mass Spectrom. Ion Processes* **1987,** *81*, 85–100.
23. Bickelhaupt, F. M.; de Koning, L. J.; Nibbering, N. M. M. Anionic Ether Cleavage of Tetrahydrofuran in the Gas Phase. *Tetrahedron* **1993,** *49*, 2077–2092.
24. Gaussian 03, Rev B.05, Frisch, M. J.; Trucks, G. W.; Schlegel, H. B.; Scuseria, G. E.; Robb, M. A.; Cheeseman, J. R.; Montgomery, J. J. A.; Vreven, T.; Kudin, K. N.; Burant, J. C.; Millam, J. M.; Iyengar, S. S.; Tomasi, J.; Barone, V.; Mennucci, B.; Cossi, M.; Scalmani, G.; Rega, N.; Petersson, G. A.; Nakatsuji, H.; Hada, M.; Ehara, M.; Toyota, K.; Fukuda, R.; Hasegawa, J.; Ishida, M.; Nakajima, T.; Honda, Y.; Kitao, O.; Nakai, H.; Klene, M.; Li, X.; Knox, J. E.; Hratchian, H. P.; Cross, J. B.; Bakken, V.; Adamo, C.; Jaramillo, J.; Gomperts, R.; Stratmann, R. E.; Yazyev, O.; Austin, A. J.; Cammi, R.; Pomelli, C.; Ochterski, J. W. A. P. Y.; Morokuma, K.; Voth, G. A.; Salvador, P.; Dannenberg, J. J.; Zakrzewski, V. G.; Dapprich, S.; Daniels, A. D.; Strain, M. C.; Farkas, O.; Malick, D. K.; Rabuck, A. D.; Raghavachari, K.; Foresman, J. B.; Ortiz, J. V.; Cui, Q.; Baboul, A. G.; Clifford, S.; Cioslowski, J.; Stefanov, B. B.; Liu, G.; Liashenko, A.; Piskorz, P.; Komaromi, I.; Martin, R. L.; Fox, D. J.; Keith, T.; Al-Laham, M. A.; Peng, C. Y.; Nanayakkara, A.; Challacombe, M.; Gill, P. M. W.; Johnson, B.; Chen, W.; Wong, M. W.; Gonzalez, C. and Pople, J. A. Gaussian, Inc.: Pittsburgh, PA, 2004.
25. Gaussian 98, Rev A.7, Frisch, M. J.; Trucks, G. W.; Schlegel, H. B.; Scuseria, G. E.; Robb, M. A.; Cheeseman, J. R.; Montgomery, J. J. A.; Vreven, T.; Kudin, K. N.; Burant, J. C.; Millam, J. M.; Iyengar, S. S.; Tomasi, J.; Barone, V.; Mennucci, B.; Cossi, M.; Scalmani, G.; Rega, N.; Petersson, G. A.; Nakatsuji, H.; Hada, M.; Ehara, M.; Toyota, K.; Fukuda, R.; Hasegawa, J.; Ishida, M.; Nakajima, T.; Honda, Y.; Kitao, O.; Nakai, H.; Klene, M.; Li, X.; Knox, J. E.; Hratchian, H. P.; Cross, J. B.; Bakken, V.; Adamo, C.; Jaramillo, J.; Gomperts, R.; Stratmann, R. E.; Yazyev, O.; Austin, A. J.; Cammi, R.; Pomelli, C.; Ochterski, J. W. A. P. Y.; Morokuma, K.; Voth, G. A.; Salvador, P.; Dannenberg, J. J.; Zakrzewski, V. G.; Dapprich, S.; Daniels, A. D.; Strain, M. C.; Farkas, O.; Malick, D. K.; Rabuck, A. D.; Raghavachari, K.; Foresman, J. B.; Ortiz, J. V.; Cui, Q.; Baboul, A. G.; Clifford, S.; Cioslowski, J.; Stefanov, B. B.; Liu, G.; Liashenko, A.; Piskorz, P.; Komaromi, I.; Martin, R. L.; Fox, D. J.; Keith, T.; Al-Laham, M. A.; Peng, C. Y.; Nanayakkara, A.; Challacombe, M.; Gill, P. M. W.; Johnson, B.; Chen, W.; Wong, M. W.; Gonzalez, C. and Pople, J. A. Gaussian, Inc.: Pittsburgh, PA, 1998.
26. Glad, S. S.; Jensen, F. Basis Set and Correlation Effects on Transition State Geometries and Kinetic Isotope Effects. *J. Phys. Chem.* **1996,** *100*, 16892–16898.
27. Gronert, S.; Keeffe, J. R. Primary Semiclassical Kinetic Hydrogen Isotope Effects in Identity Carbon-to-Carbon Proton- and Hydride-Transfer Reactions, an ab Initio and DFT Computational Study. *J. Org. Chem.* **2006,** *71*, 5959–5968.
28. Hiraoka, K.; Fujita, K.; Ishida, M.; Ichikawa, T.; Okada, H.; Hiizumi, K.; Wada, A.; Takao, K. Gas-Phase Ion/Molecule Reactions in C_5F_8. *J. Phys. Chem. A* **2005,** *109*, 1049–1056.
29. McAllister, M. A. Characterization of Low-Barrier Hydrogen Bonds. 2. HF_2^-: A density functional and ab Initio study. *THEOCHEM* **1998,** *427*, 39–53.
30. Su, T.; Chesnavich, W. J. Parametrization of the Ion-Polar Molecule Collision Rate Constant by Trajectory Calculations. *J. Chem. Phys.* **1982,** *76*, 5183–5185.
31. Miller, K. J.; Savchik, J. A New Empirical Method to Calculate Average Molecular Polarizabilities. *J. Am. Chem. Soc.* **1979,** *101*, 7206–7213.
32. *CRC Handbook of Chemistry and Physics, 75th ed.*; Lide, D. R., Ed.; CRC Press: Boca Raton, FL, 1994, pp. 9–49, 10–200.
33. Chase, W. M., Jr.; Davies, C. A.; Downey, J. J. R.; Frurip, D. J.; McDonald, R. A.; Syverud, A. N. JANAF Thermochemical Tables, 3rd ed. Parts I and II. *J. Phys. Chem. Ref. Data* **1985,** Suppl 1.
34. Linstrom, P. J., Mallard, W. G. NIST Chemistry WebBook, NIST Standard Reference Database Number 69, June 2005, National Institute of Standards and Technology: Gaithersburg, MD, 20899 (http://webbook.nist.gov).
35. Bohme, D. K.; Raksit, A. B. Gas-Phase Measurements of the Influence of Stepwise Solvation on the Kinetics of S_N2 Reactions of Solvated Fluoride Ion with Methyl Chloride and Methyl Bromide and of Solvated Chloride Ion with Methyl Bromide. *Can. J. Chem.* **1985,** *63*, 3007.
36. Westheimer, F. H. The Magnitude of the Primary Kinetic Isotope Effect for Compounds of Hydrogen and Deuterium. *Chem. Rev.* **1961,** *61*, 265–273.
37. Sun, L.; Song, K.; Hase, W. L. An S_N2 Reaction That Avoids Its Deep Potential Energy Minimum. *Science* **2002,** *296*, 875–878.
38. Baer, T.; Hase, W. L. Unimolecular Reaction Dynamics: Theory and Experiment; Oxford University Press: New York, 1996, pp. 1–448.